

Analytical Calculation of the Average Dancoff Factor for a Fuel Kernel in a Pebble Bed High-Temperature Reactor

E. E. Bende* and A. H. Hogenbirk

NRG, P.O. Box 25, 1755 ZG Petten, The Netherlands

and

J. L. Kloosterman and H. van Dam

Delft University of Technology, Interfaculty Reactor Institute
Mekelweg 15, 2629 JB Delft, The Netherlands

Received September 1, 1998

Accepted February 2, 1999

Abstract—An analytical expression was derived for the average Dancoff factor of a fuel kernel (C^{fk}) in a pebble of a high-temperature gas-cooled reactor. This Dancoff factor accounts for the probability that a neutron escaping from a fuel kernel enters another fuel kernel, in the same pebble or in other pebbles, without colliding with a moderator nucleus in between. If the fuel zone of the pebble is thought to be of infinite dimensions, the Dancoff factor becomes equal to the so-called infinite-medium Dancoff factor C_{∞}^{fk} . The C_{∞}^{fk} has been determined by the evaluation of three existing analytical expressions and by two Monte Carlo calculations performed with the MCNP-4A code, for various coated-particle densities. The Dancoff factor C^{fk} can be written as C_{∞}^{fk} times a correction factor. The latter has been calculated for different fuel zone radii and pebble shell thicknesses. For the standard pebble, C^{fk} as a function of the number of coated particles has been calculated both analytically and with MCNP. The results of both methods are in good agreement. The analytical calculation method is preferred because it consumes practically no CPU time and obviates the building of MCNP models.

I. INTRODUCTION

A pebble bed-type high-temperature reactor (HTR) is fueled with 6-cm-diam graphite spherical fuel elements. Within these pebbles one can distinguish an outer fuel-free spherical shell ($2.5 < R < 3$ cm) and a fuel zone ($R < 2.5$ cm), in which tens of thousands of tiny coated fuel particles are embedded. A pile of pebbles can be considered a double-heterogeneous system. The first heterogeneity, on the smallest geometric scale, is the fuel kernel that is surrounded by the coating layers and graphite matrix successively. The second one is the heterogeneity of the fuel zone and the pebble shell.

A standard calculational scheme starts with the preparation of group cross sections on the finest geometric

scale, which in the case of an HTR would be the fuel kernel surrounded by coating layers and graphite. The structure on this elementary level is then translated into a unit cell, which, for instance, could be a spherical multi-region unit cell with white-boundary conditions, in which the thermalization and neutron slowing-down problems are treated.

The resonance absorption is usually calculated by the collision probability method applied for a unit cell with a fuel and moderator region. For such a two-region unit cell, the neutron slowing-down process can be described by two coupled integral equations, as originally proposed by Chernick.¹ By assuming flat sources in both the fuel and the moderator regions, applying the reciprocity theorem, and assuming a $1/E$ flux in the moderator, these two coupled equations reduce to a single slowing-down equation for the energy-dependent flux in the fuel region

*E-mail: bende@nrg-nl.com

(see many textbooks, for example, Ref. 2, p. 430). The numerical integration of this equation,³ with respect to the energy-dependent flux, is referred to as the Nordheim integral method.⁴

With the energy-dependent flux, the shielded group cross sections can be generated [i.e. $\bar{\sigma} = \int \sigma(E)\phi(E) dE / \int \phi(E) dE$]. The integral equation depends among others on the escape probability P_F , which is the probability that a neutron originating in the fuel region (homogeneously and isotropically) will reach the surface of the lump without any collisions in the fuel region. For simple geometries, including a sphere, analytical expressions for P_F given by Case, de Hoffmann, and Placzek⁵ have been built in in many codes.

For a single lump in an infinite moderator, the neutron that escapes from the lump will obviously have its next collision in the moderator. However, if the distance between lumps is not large compared to the mean free path (mfp) of the moderator, the possibility exists that a neutron escaping from a fuel lump hits another fuel lump without a collision in the moderator in between. The distance between fuel kernels in an HTR pebble is typically of the order of millimetres, while the mfp of graphite at resonance energies is ~ 2.5 cm, which implies that the kernels influence each other. To account for this effect, one must replace or modify the escape probability P_F .

Teuchert⁶ and Teuchert and Breitbarth⁷ developed an escape probability $P_F(\sigma)$ for double-heterogeneous systems (coated particles in rods and spheres). The double-heterogeneous $P_F(\sigma)$ is calculated by a collection of analytical and numerical integrations, which were implemented in the ZUT resonance-treatment code.^{8,9} Because the double-heterogeneous escape probability $P_F(\sigma)$ depends on the total cross section of the absorber, which of course varies strongly with energy, it has to be recalculated continuously with varying energy.

A different approach that obviates the modification of codes is to adopt Nordheim's well-known effective or Dancoff-corrected escape probability (in Ref. 3 or p. 434 of Ref. 2), which is already incorporated in many codes, and to account for the double-heterogeneity via the so-called Dancoff(-Ginsburg) factor. The effective escape probability reads as follows:

$$P_F^* = P_F \cdot \frac{1 - C}{1 - C(1 - \Sigma_i^F \bar{l}_F P_F)} \quad (1)$$

where

Σ_i^F = energy-dependent total macroscopic cross section of the fuel

\bar{l}_F = mean chord length ($4 \times$ volume/surface for convex bodies⁵) of the fuel kernel

C = Dancoff factor.

In the case of an HTR, P_F is the (single-heterogeneous) probability to escape from a single fuel kernel. The Dancoff factor in Eq. (1) should account for fuel kernel shadowing in a double-heterogeneous sense. It depends only on the geometry of the system and on the total macroscopic cross section of the moderator. Because the latter hardly varies in the resonance range, the Dancoff factor is usually calculated only once.

II. CALCULATION OF DANCOFF FACTORS

The Dancoff factor can be calculated by averaging the Dancoff factors of individual fuel kernels. The Dancoff factor for an individual kernel is the probability that a neutron escaping in a random direction from the kernel enters another kernel, either in the same or in another pebble, without a collision in the moderator in between.

Equation (1) takes care of the possibility that neutrons may traverse more than one fuel kernel before it collides with a moderator nucleus. It is strictly correct if the absorber lumps are randomly distributed,^{3,10} which is the case for the coated particles in the graphite matrix. Note that if Wigner's rational approximation¹¹ [i.e., $P_F = (1 + \Sigma_i^F \bar{l}_F)^{-1}$] is inserted into Eq. (1), one also obtains for the Dancoff-corrected escape probability the Wigner form, namely, $P_F^* = (1 + \Sigma_i^F \bar{l}_F^*)^{-1}$, but with a corrected mean chord length $\bar{l}_F^* = \bar{l}_F / (1 - C)$. This correction can be seen as a reduction of the surface of the lump by a factor $(1 - C)$ if the volume of the lump is thought to be constant. This was originally introduced by Dancoff and Ginsburg,¹² although they formulated the lump-lump interaction in another way.¹³

For simple lattice cells, the Dancoff factor is usually internally calculated by the resonance-shielding code. However, if the geometry is more complicated, it has to be given as an input parameter. To calculate Dancoff factors in irregular geometries, researchers have developed some codes. The DANCOFF-MC code,^{13,14} based on the Monte Carlo method, can calculate Dancoff factors in an arbitrary arrangement of cylindrical pins or spherical fuel elements. However, in case of the HTR pebble, it only accounts for fuel kernel interactions within a single pebble.¹⁵ The MCNP-4A Monte Carlo code¹⁶ offers the possibility of modeling all kinds of complex geometries in which Dancoff factors can be calculated by using a special option.¹⁷ However, as will be seen later, there are some modeling restrictions; moreover, in the case of the HTR, the MCNP calculation requires a great deal of computing time.

In this paper, an analytical expression for the average fuel kernel Dancoff factor, which accounts for the double heterogeneity, is presented. For various fuel pebble specifications, the analytical Dancoff factors are computed by a FORTRAN code and compared to those obtained by MCNP calculations.

III. TRANSLATION FROM PEBBLE GEOMETRY TO EQUIVALENT UNIT CELLS

The pebble bed-type HTR consists of a helium-cooled core that is filled with 3-cm-radius graphite spherical fuel elements (pebbles). In power reactors these pebbles are stochastically stacked, which implies that they occupy $\sim 62\%$ of the core volume.¹⁸ The fuel pebbles in the core are sometimes mixed with moderator pebbles, which consist of graphite only. The startup core of the modular¹⁹ HTR-M consists, for example, of 50% fuel pebbles and 50% moderator pebbles.

Figure 1 shows a cross section of a fuel pebble. In each fuel pebble,²⁰ tens of thousands of coated fuel particles are dispersed in the 2.5-cm-radius fuel zone. The standard coated particle, which has been used for >20 yr, is the one with the so-called TRISO coating layer.²¹ Such a coated particle comprises an oxide fuel kernel surrounded successively by a porous graphite buffer layer, a pyrolytic carbon (PyC) layer, a silicon carbon (SiC) layer, and again a pyrolytic carbon layer with thicknesses of 95, 40, 35, and 40 μm , respectively.

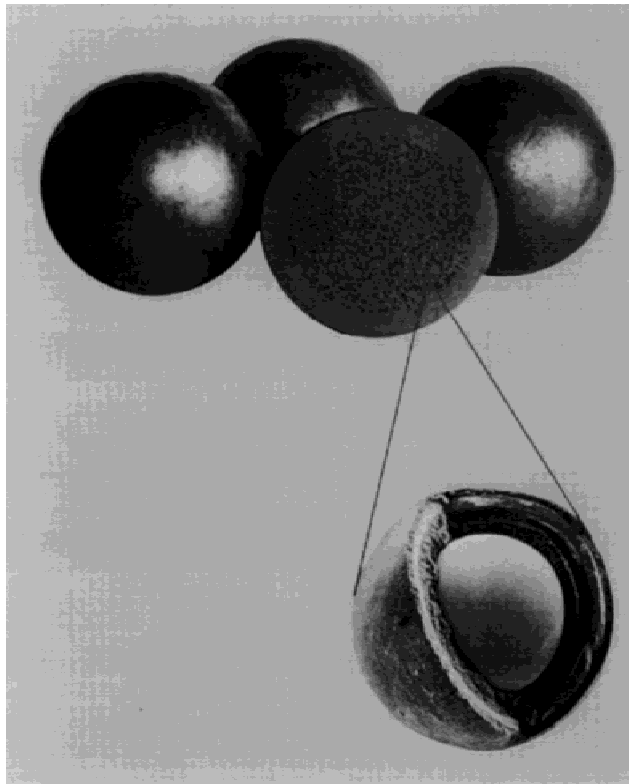


Fig. 1. The HTR fuel element containing $\sim 12\,000$ coated particles. The coated particles are randomly dispersed in the 5-cm-diam fuel zone of the pebble. One of the coated particles is magnified, which reveals that it is composed of a fuel kernel surrounded by several coating layers.

The porous buffer provides the free volume for fission and reaction gases.

The PyC and SiC layers are capable of essentially complete retention of gaseous fission products. Moreover, the SiC layer acts as a barrier to prevent the escape of metallic fission products, in particular, and provides mechanical strength to TRISO coated particles. The coated fuel kernel usually has a 250- μm radius, but for the purpose of plutonium burning,²² kernels with radii varying from 100 to 110 μm have been fabricated and tested.²³ Both fuel kernel types are considered in this paper.

For calculational purposes, the heterogeneity of the fuel kernel surrounded by the coatings and graphite matrix is translated into a grain cell. On this geometric level, the resonance-shielding calculations take place, and hence, a Dancoff factor for the fuel kernel has to be provided. For the analytical calculation of this Dancoff factor, we consider an equivalent spherical unit cell with white-boundary conditions, which seems expedient for a random distribution of coated particles. This grain cell consists of an inner sphere with radius r_1 , which corresponds to the fuel kernel, and a spherical shell with outer radius r_2 , which contains the coating layers and the graphite matrix, homogeneously mixed.

The stochastically stacked pile of fuel pebbles is also modeled as a spherical two-region unit cell with white-boundary conditions. This equivalent pebble cell consists of an inner sphere, representing the fuel zone of the pebble, with radius R_1 of 2.5 cm, and an outer spherical shell with outer radius R_2 . The outer shell contains a homogeneous mixture of the 0.5-cm pebble shell, the moderator balls if present, and possibly the void between the pebbles. The radius R_2 is determined by the volume occupied by the aforementioned materials. In the absence of moderator balls, one obtains $R_2 = 3$ cm if the void between the pebbles is neglected or $R_2 = 3.52$ cm if the void and pebble shell are merged. In the latter case, the shell of the unit cell contains graphite with a lower density than that of the actual 0.5-cm pebble shell.

The preceding consideration shows that the heterogeneity of the fuel kernel in the graphite matrix, as well as the heterogeneity of the spherical fuel zone of the pebble with the surrounding amount of graphite (shell and moderator pebbles), is translated into equivalent spherical two-region white-boundary unit cells. Of course, these two unit cells differ with respect to radii and macroscopic cross section of the outer spherical shell. Hereafter, the parameters corresponding to the grain cell are written with lower-case letters, while those of the pebble cell are written with upper-case letters.

IV. TRANSMISSION PROBABILITIES IN A TWO-REGION WHITE-BOUNDARY UNIT CELL

The first-flight escape and transmission probabilities for a spherical white-boundary unit cell have been

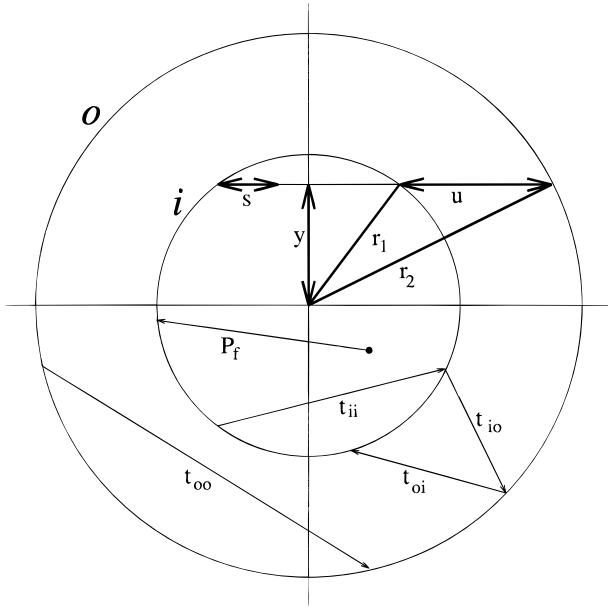


Fig. 2. A spherical two-region unit cell (grain cell) with white-boundary conditions. The inner and outer boundaries are denoted by *i* and *o*, respectively. The upper half-plane shows the parameters that are used in the various integrals. In the lower half-plane, the first-flight escape probability P_F and various transmission probabilities are depicted. By replacing the lower-case parameters by their upper-case counterparts, the figure becomes applicable to the pebble cell.

derived by Westfall.²⁴ Figure 2 shows that the equivalent spherical two-region grain cell is characterized by the radius of the inner sphere r_1 and by the outer radius of the spherical shell r_2 . The surfaces of the inner and outer zones are denoted by *i* and *o*, respectively. The total macroscopic cross section of the outer spherical shell reads Σ_t^m . For the pebble cell these parameters are replaced according to $(r_1, r_2, \Sigma_t^m, i, o) \rightarrow (R_1, R_2, \Sigma_t^M, I, O)$. The surfaces are treated as white boundaries, which means that uniformly distributed isotropic sources with corresponding cosine currents are assumed at the interfaces. The transmission probabilities that can be distinguished for the mentioned geometry read as follows:

1. t_{io} is the probability that a neutron that leaves the inner boundary isotropically reaches the outer boundary without collisions.
2. t_{oi} is the probability that a neutron that leaves the outer boundary isotropically reaches the inner boundary without collisions.
3. t_{oo} is the probability that a neutron that leaves the outer boundary isotropically reaches again the outer boundary without collisions and without passing through the inner region.

4. t_{ii} is the probability that a neutron that leaves the inner boundary isotropically reaches again the inner boundary without collisions and without passing through the outer region.

For the white-boundary condition mentioned earlier, t_{io} is given by

$$t_{io} = \frac{\int ds \int_{\hat{n} \cdot \hat{\Omega} > 0} d\Omega \hat{n} \cdot \hat{\Omega} \exp[-\Sigma_t^m l(\vec{r}, \hat{\Omega})]}{\int ds \int_{\hat{n} \cdot \hat{\Omega} > 0} d\Omega \hat{n} \cdot \hat{\Omega}}, \quad (2)$$

where

l = length of a vector with direction $\hat{\Omega}$ leading from the surface point \vec{r} on surface *i* through the outer spherical shell to surface *o*

Σ_t^m = total macroscopic cross section of the outer spherical shell

\hat{n} = normal vector on surface *i* in the point \vec{r} .

The integrals extend in $\hat{\Omega}$ over all angles $\hat{n} \cdot \hat{\Omega} > 0$ and in \vec{r} over surface *i*. Because of the spherical symmetry, the double integral of Eq. (2) can be reduced²⁵ to

$$t_{io} = \frac{\int_0^{r_1} dy 2\pi y \exp[-\Sigma_t^m u]}{\int_0^{r_1} dy 2\pi y} = \frac{1}{\pi r_1^2} \int_0^{r_1} dy 2\pi y \exp[-\Sigma_t^m u], \quad (3)$$

where only the integration over variable y has to be carried out. The variables y and $u = \sqrt{r_2^2 - y^2} - \sqrt{r_1^2 - y^2}$ are shown in Fig. 2. In this new representation, the problem is reduced to one in which only neutron paths parallel to the x axis have to be considered.

To avoid cumbersome integrals in the remainder of this paper, we introduce

$$\tau_{r_a, r_b}^{r_c, r_d} \equiv \frac{\int_{r_c}^{r_d} dy 2\pi y \circ}{\int_{r_a}^{r_b} dy 2\pi y \cdot 1} = \frac{1}{r_b^2 - r_a^2} \int_{r_c}^{r_d} dy 2y \circ, \quad (4)$$

which is an integral operator that has to act on a particular operand. The latter is usually the probability that a neutron moves a distance without any interaction and is usually of the form $\exp[-\Sigma l(y)]$, where Σ is a macroscopic cross section and l a certain distance, that is, a function of parameter y . With this tool the transmission probabilities through the spherical shell, including their final form given by Westfall, read as follows:

$$\begin{aligned}
 t_{io} &= \tau_{0,r_1}^{0,r_1} \circ \exp[-\Sigma_t^m u] \\
 &= \frac{1}{2(r_1 \Sigma_t^m)^2} \left[(a+1)e^{-a} - (b+1)e^{-b} \right. \\
 &\quad \left. + \frac{a^4}{b^2} E_3(b) - a^2 E_3(a) \right], \quad (5)
 \end{aligned}$$

$$t_{oi} = \tau_{0,r_2}^{0,r_1} \circ \exp[-\Sigma_t^m u] = \left(\frac{r_1}{r_2}\right)^2 t_{io}, \quad (6)$$

and

$$\begin{aligned}
 t_{oo} &= \tau_{0,r_2}^{r_1,r_2} \circ \exp[-\Sigma_t^m \sqrt{r_2^2 - y^2}] \\
 &= \frac{1}{2(r_2 \Sigma_t^m)^2} [1 - (1 + 2a)\exp(-2a)], \quad (7)
 \end{aligned}$$

in which E_3 is the exponential-integral function of the third order²⁶ and

$$a = \Sigma_t^m \sqrt{r_2^2 - r_1^2} \quad \text{and} \quad b = \Sigma_t^m (r_2 - r_1). \quad (8)$$

The first-flight escape probability for a sphere with radius r_1 has been given by Case, de Hoffmann, and Placzek⁵ and reads as follows:

$$\begin{aligned}
 P_F &= \mathcal{P}_{r_1} \circ \exp[-s \Sigma_t^F] \\
 &= \frac{3}{4\lambda} \left[1 - \frac{1}{2\lambda^2} \{1 - (1 + 2\lambda)e^{-2\lambda}\} \right], \quad (9)
 \end{aligned}$$

where Σ_t^F is the total macroscopic cross section of the inner region $\lambda = \Sigma_t^F r_1$ and where \mathcal{P}_{r_1} is an integral operator, defined as

$$\mathcal{P}_{r_1} \equiv \frac{\int_0^{r_1} dy \, 2\pi y \int_0^{2\sqrt{r_1^2 - y^2}} ds \circ}{\int_0^{r_1} dy \, 2\pi y \int_0^{2\sqrt{r_1^2 - y^2}} ds \cdot 1}. \quad (10)$$

Here, the integration over the entire volume of the inner sphere in Fig. 2 is accounted for by the double integral over the variables y and s . For any convex lump the transmission probability through the lump³ can be expressed as

$$t_{ii} = 1 - \bar{l}_F \Sigma_t^F P_F, \quad (11)$$

where \bar{l}_F is the mean chord length of the lump, which equals $\frac{4}{3}r_1$ for a sphere.

V. DANCOFF FACTOR FOR A RANDOM DISTRIBUTION OF FUEL KERNELS IN AN INFINITE MEDIUM

The Dancoff factor accounts for the probability that a neutron that leaves an absorber lump passes through

the moderator without collisions and enters another absorber lump. In an infinite medium in which fuel kernels are randomly distributed in the moderator, the Dancoff factor is given by the summation of the probabilities for neutrons to enter a particular fuel kernel positioned at a particular distance, before making a collision.

In the invariant embedding theory,²⁵ the distance covered by a neutron from absorber lump to absorber lump corresponds to that in a unit cell, allowing for a number of reflections at its white boundary. The probability that a neutron will leave the surface of the fuel kernel isotropically, pass through the moderator without collisions, and reach the white boundary o of the unit cell is equal to t_{io} . The probability that it will move n times from the outer white boundary to the same boundary without collisions and without passing through a kernel is $(t_{oo})^n$. The probability that, after the last isotropic reflection at the white boundary o , the neutron will reenter a fuel kernel without collisions in the moderator reads t_{oi} . The Dancoff factor of the infinite medium is equal to the probability that a neutron leaving the fuel kernel will reach another fuel kernel without collisions with moderator nuclei after an arbitrary number of reflections at the white boundary o and hence reads²⁵ as follows:

$$C_\infty^{fk} = \sum_{n=0}^{\infty} t_{io} t_{oo}^n t_{oi} = \frac{t_{io} t_{oi}}{1 - t_{oo}}. \quad (12)$$

Equations (5), (6), and (7) show that C_∞^{fk} can be expressed as a function of two parameters, e.g., $\Sigma_t^m r_1$ and r_2/r_1 . The transmission probabilities of Eqs. (5), (6), and (7) are also programmed in SCALE (Sec. F.2.3.7 of Ref. 27). However, these are used to calculate the first-flight escape probability of annular spherical pellets and are unfortunately not used to calculate the Dancoff factor. Instead, SCALE uses routines taken from the SUPERDAN program,²⁸ which uses a double-numerical integration to analytically determine Dancoff factors. It accounts for the overshadowing of lumps up to and including the third nearest neighbors in a lattice. Because the algorithms were observed to be inadequate in some applications, in SCALE a correction factor has been added to the Dancoff factor to treat the interaction of all subsequent neighbors (Sec. M.7.2.5.3 of Ref. 27). However, for the purpose of tiny fuel kernels dispersed in graphite with a large number of equivalent unit cells per mfp, this approximation gives questionable values.^{15,17}

Janssen²⁵ derived from the exact expression of Eq. (12) a rational approximation for C_∞^{fk} , which reads

$$C_\infty^{fk} = \frac{1}{1 + \Sigma_t^m \bar{l}_M}, \quad (13)$$

where \bar{l}_M is a sort of a mean chord length of the moderator region, defined as

$$\bar{l}_M = \frac{4V_M}{S_F} = \frac{4 \cdot \frac{4}{3}\pi(r_2^3 - r_1^3)}{4\pi r_1^2}. \quad (14)$$

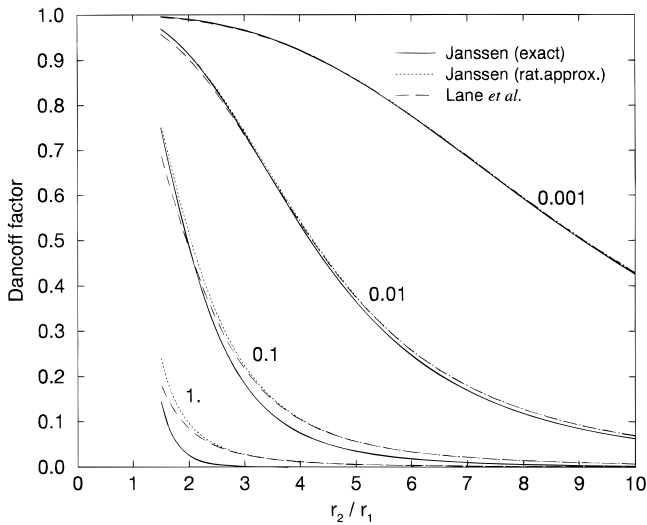


Fig. 3. The Dancoff factor for a spherical two-region unit cell as a function of r_2/r_1 with $\Sigma^m r_1$ as a parameter, calculated by three methods. The solid, dotted, and dashed lines are calculated with Eq. (12), Eqs. (13) and (14), and Eqs. (13) and (15), respectively.

In the limits of $r_2/r_1 \rightarrow 1$ and $r_2/r_1 \rightarrow \infty$, the rational approximation equals the exact expression of Eq. (12). A rather simple analytic method described by Lane, Nordheim, and Sampson¹⁰ yields for the Dancoff factor of the infinite medium with a random kernel distribution the same expression as that of Eq. (13), except that \bar{l}_M is now given by

$$\bar{l}_M = \frac{4(V_M + V_F)}{S_F} = \frac{4 \cdot \frac{4}{3} \pi r_2^3}{4 \pi r_1^2} \quad (15)$$

Their method is justified in the case of high dilution of the fuel kernels; that is, the volume fraction of the fuel should be small. This means that $V_F \ll V_M$, and hence, \bar{l}_M of Eq. (15) tends to that of Eq. (14). Figure 3 shows the Dancoff factor as a function r_2/r_1 , with $\Sigma^m r_1$ as a parameter calculated on the one hand by the exact expression of Janssen [Eq. (12)] and on the other by Eq. (13) with for \bar{l}_M the expressions of Janssen [Eq. (14)] and Lane, Nordheim, and Sampson [Eq. (15)].

VI. TRANSMISSION PROBABILITIES IN A DOUBLE-HETEROGENEOUS SYSTEM

The resonance self-shielding calculations are performed at the level of the grain cell. In this calculation a Dancoff factor is needed that accounts for the effect of neighboring fuel kernels as well as for fuel kernels in other pebbles. This Dancoff factor can therefore be calculated as the sum of two probabilities. The first is the probability that a neutron leaving a fuel kernel will enter

another kernel without any collision in the moderator within the same pebble, which will be designated the intrapebble Dancoff factor C_{intra} . The other is the probability that a neutron leaving a particular kernel will enter a fuel kernel in another pebble without collisions in the moderator, which will be designated as the interpebble Dancoff factor C_{inter} . The latter is usually much smaller than the first one, which is basically due to the neutron's increased probability to collide with a nucleus of the graphite in the pebble shell (and in some cases the moderator pebbles), which it has to pass through.

Figure 4 shows a schematic overview of the double-heterogeneous medium with three trajectories—in which a neutron that leaves a fuel kernel finally ends up in another kernel—that are typical for all possible histories. The arrow $T_{ii'}$ in Fig. 4 corresponds to the transmission probability of a neutron leaving a fuel kernel (with white boundary i) and entering the white boundary (i') of another fuel kernel in the same pebble, which hence contributes to the intrapebble Dancoff factor. The intrapebble Dancoff factor accounts for the set of paths between all possible pairs of kernels within the same pebble, which can be calculated by a double summation of $T_{ii'}$ over i and i' .

The other two histories contribute to the interpebble Dancoff factor. The four arrows denoted by T_{ii} , T_{IO} , T_{OI} , and T_{ii} in Fig. 4 correspond to the history in which a neutron leaves the white boundary i of a fuel kernel, reaches

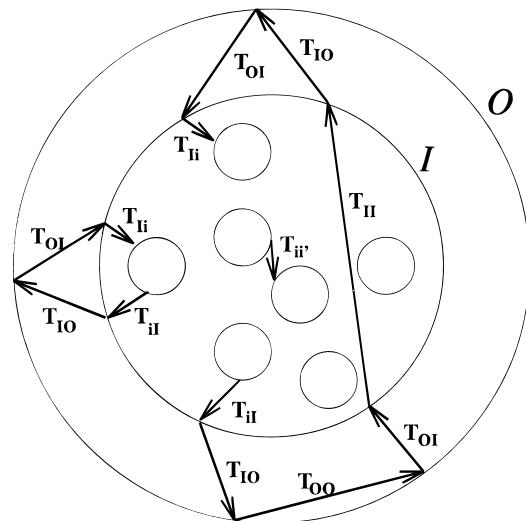


Fig. 4. Schematic overview of the double-heterogeneous spherical system. The first heterogeneity is that of the fuel kernels, which are surrounded by the graphite matrix. The second one is the fuel zone of the pebble that is surrounded by a graphite shell. Three exemplifying neutron trajectories are shown. The one denoted $T_{ii'}$ contributes to the intrapebble Dancoff factor, while the other two contribute to the interpebble Dancoff factor.

the white boundary I at which it is isotropically transmitted, reaches the white boundary O at which it is isotropically reflected, reaches again the white boundary I of another pebble at which it is isotropically transmitted in the direction of the pebble's fuel zone, and hits a fuel kernel with white boundary i , successively. This means that the neutron finally enters a fuel kernel of a neighboring pebble without any collision with a graphite nucleus.

The concatenation of arrows denoted by $T_{iI}-T_{IO}-T_{OO}-T_{OI}-T_{II}-T_{IO}-T_{OI}-T_{II}$ corresponds to a history in which a neutron escapes from the first pebble ($T_{iI}-T_{IO}$), passes through the shell (T_{OO}) of a second one, passes successively through the shell, fuel zone, and again shell ($T_{OI}-T_{II}-T_{IO}$) of a third pebble without collisions and without crossing any kernel, and finally enters the fourth pebble at which it eventually impinges on a fuel kernel ($T_{OI}-T_{II}$).

These two histories form only a subset of the infinite number of histories that contribute to the interpebble Dancoff factor. An arbitrary history contributing to C_{inter} is minimally built up by the product of four factors: the probability of escaping from the fuel zone of the initial pebble (T_{iI}), the probability of escaping from the pebble shell (T_{IO}), the probability of reaching the surface of the fuel zone of the final pebble (T_{OI}), and the probability of entering a fuel kernel in this fuel region (T_{ii}).

This basic history is extended if between the departure from the initial pebble and the arrival at the final pebble, the neutron crosses i times the shells of intermediate pebbles (T_{OO}) ^{i} and, moreover, passes j times through complete pebbles ($T_{OI}T_{II}T_{IO}$) ^{j} . The interpebble Dancoff factor accounts for all possible combinations and hence reads

$$C_{inter} = T_{iI}T_{IO}[1 + T_{OO} + T_{OO}^2 + \dots] \times \{1 + (T_{OI}T_{II}T_{IO}) + (T_{OI}T_{II}T_{IO})^2 + \dots\}T_{OI}T_{ii} \quad (16)$$

in which the series between the square brackets and the braces corresponds to transmissions through shells of pebbles and through complete pebbles, respectively. By progression of the series and rearrangement of the terms, one can write Eq. (16) as

$$C_{inter} = \frac{T_{IO}T_{OI}}{1 - T_{OO}} \frac{T_{iI}T_{ii}}{1 - T_{OI}T_{II}T_{IO}} \quad (17)$$

where the first fraction can be identified through Eq. (12) as the infinite-medium Dancoff factor of the pebble fuel zone, which leads to the introduction of

$$C_{\infty}^{FZ} = \frac{T_{IO}T_{OI}}{1 - T_{OO}} \quad (18)$$

The (upper-case) transmission probabilities are equal to those of Eqs. (5), (6), and (7) except that the parameters (Σ_t^m, r_1, r_2) have to be replaced by (Σ_t^M, R_1, R_2), which

are the total macroscopic cross section of the outer spherical shell, and the inner radius and the outer radius of the equivalent pebble cell, respectively.

The total Dancoff factor for the fuel kernel in the double-heterogeneous system now becomes

$$C^{fk} = C_{intra} + C_{\infty}^{FZ} \frac{T_{ii}T_{ii}}{1 - T_{ii}T_{IO}T_{OI}} \quad (19)$$

Note that Eq. (19) not only is valid for an HTR pebble but also is applicable to other double-heterogeneous systems, such as the so-called sphere-pac light water reactor fuel rod. The transmission probabilities in Eq. (19) depend of course on the geometry under consideration.

VII. CALCULATION OF THE DANCOFF FACTOR

As mentioned previously, the Dancoff factor is equal to the sum of the inter- and intrapebble Dancoff factors. These will be evaluated successively.

VII.A. The Intrapebble Dancoff Factor

To calculate the intrapebble Dancoff factor, one assumes that each kernel emits as many neutrons as the others and because the kernels are distributed randomly, the fuel region of the pebble can be considered as containing a uniform source distribution. To account for this uniform source distribution, one must carry out an integration over the volume of the pebble fuel region. The integrand is then equal to the probability that a neutron, departing from coordinates (s, y) and subsequently moving parallel to the horizontal axis in Fig. 2, will enter a fuel kernel before it reaches surface I of the fuel region. Distance s , which the neutron can travel before it reaches the surface of the fuel region, assuming that the neutron moves in the negative x direction in Fig. 2, corresponds to a certain number of unit cells that will be passed through. The average number of grain cells that is traversed between the departure and arrival cells is given by distance s' divided by the mean chord length of a single grain cell. Here, $s' = s - \bar{l}_{gc}$, which is the actual distance s corrected for the average distance that the neutron travels in the departure and arrival cells together (\bar{l}_{gc}).

If the number of unit cells that is crossed, without colliding with a moderator nucleus and without crossing a fuel kernel, is equal to $n - 1$ given by s'/\bar{l}_{gc} , one can see that $n = s/\bar{l}_{gc}$. Considering a neutron trace in which maximally $n - 1$ grain cells are traversed, the corresponding probability of leaving a kernel and entering another kernel within the distance of s reads $t_{io}(1 + t_{oo} + \dots + t_{oo}^{n-1})t_{oi}$. This series can be written as $[t_{io}t_{oi}/(1 - t_{oo})](1 - t_{oo}^n)$.

Analogously to the calculation of the first-flight escape probability according to Eq. (9), the intrapebble Dancoff factor now becomes

$$C_{intra} = \mathcal{P}_{R_1} \circ \left[\frac{t_{io} t_{oi}}{1 - t_{oo}} (1 - t_{oo}^n) \right] \\ = \frac{t_{io} t_{oi}}{1 - t_{oo}} [1 - \mathcal{P}_{R_1} \circ t_{oo}^n] , \quad (20)$$

where \mathcal{P}_{R_1} is defined in Eq. (10). The fraction in front of the term between the square brackets at the right side of Eq. (20) is equal to the infinite-medium Dancoff factor for a fuel kernel (i.e., C_{∞}^{fk}).

If we replace the integer n by the equivalent real number s/\bar{l}_{gc} , the integral part of Eq. (20) can be written as

$$\mathcal{P}_{R_1} \circ t_{oo}^n = \mathcal{P}_{R_1} \circ \exp \left[- \left(\frac{-\ln t_{oo}}{\bar{l}_{gc}} \right) s \right] . \quad (21)$$

Comparing this to Eq. (9) leads to the introduction of the pseudo cross section

$$\Sigma^* \equiv \left(\frac{-\ln t_{oo}}{\bar{l}_{gc}} \right) . \quad (22)$$

This pseudo cross section can physically be interpreted as the probability per unit path length traveled that a neutron will either collide with a moderator nucleus or will enter a fuel kernel. Note that in the absence of moderator material between the kernels, the pseudo cross section is not zero; rather, it reads as follows:

$$\Sigma^* \rightarrow -\frac{1}{\frac{4}{3}r_2} \ln \left[1 - \left(\frac{r_1}{r_2} \right)^2 \right] , \quad (23)$$

where the ($\Sigma_i^m \rightarrow 0$) limit of Eq. (7) has been used. If the kernels occupy only a small volume of the fuel zone, which implies that $r_1/r_2 \ll 1$, one obtains $\Sigma^* = \pi r_1^2 / (\frac{4}{3}\pi r_2^3)$. This pseudo macroscopic cross section is now equal to the kernel density $1/(\frac{4}{3}\pi r_2^3)$ times the microscopic cross section πr_1^2 of a kernel. The reciprocal of this Σ^* is in agreement with Lane, Nordheim, and Sampson's expression¹⁰ for the mfp between kernels if the moderator were not present.

Another interesting case is the limit of very small kernels, but now with the moderator material between them. In the limit of $r_1/r_2 \rightarrow 0$, the expected result of $\Sigma^* \rightarrow \Sigma_i^m$ is found. Combining Eqs. (20), (21), and (22) gives analogously to Eq. (9) the following:

$$C_{intra} = C_{\infty}^{fk} [1 - P_F(\Sigma^* R_1)] . \quad (24)$$

Equation (24) shows that the intrapebble Dancoff factor is equal to the Dancoff factor for the (single-heterogeneous) infinite medium C_{∞}^{fk} corrected for the probability that the neutron leaves the fuel zone of the pebble. This probability is similar to the first-flight escape probability P_F of a sphere. However, its argument is now the pseudo cross sec-

tion Σ^* times the radius of the fuel zone R_1 , which can be written as

$$\Sigma^* R_1 = (-\ln t_{oo}) \frac{R_1}{\bar{l}_{gc}} = \frac{3}{4} (-\ln t_{oo}) N_{gr}^{1/3} , \quad (25)$$

where we have used the fact that the mean chord length of the grain cell is equal to $\frac{4}{3}r_2$ and that the volume of the fuel zone $\frac{4}{3}\pi R_1^3$ divided by the volume of a grain cell $\frac{4}{3}\pi r_2^3$ is equal to the number of grains in the fuel zone N_{gr} . Note that in the limit of $R_1 \rightarrow \infty$, while Σ^* remains constant, the intrapebble Dancoff factor becomes equal to the infinite-medium Dancoff factor C_{∞}^{fk} .

VII.B. The Interpebble Dancoff Factor

According to Eq. (19) the interpebble Dancoff factor is equal to the product of two terms. The first term is the infinite-medium Dancoff factor for the fuel zone of a pebble. The second term depends on the transmission probabilities T_{IO} , T_{OI} , T_{iI} , T_{Ii} , and T_{II} , where the first two can be calculated by Eqs. (5) through (8). The last one is the transmission probability that a neutron leaving isotropically the surface I of the fuel region will reach this surface again without colliding with a moderator nucleus and without passing through a kernel. It can be calculated by integrating the probability t_{oo}^n along chords from one point on surface I to another point on surface I , where the directions of the chords are again isotropically distributed. Here, t_{oo} is the probability that a neutron traverses a grain cell without collisions with a moderator nucleus and without crossing a fuel kernel, and n is the number of grain cells the neutron has to traverse from one point on surface I to the other point on surface I . The latter is again given by the distance the neutron has to move divided by the mean chord length of a grain cell.

Figure 2 shows that the length of the straight line along which the neutron moves from inner surface to inner surface, parallel to the horizontal axis, is equal to $2\sqrt{R_1^2 - y^2}$. Therefore, the probability t_{oo}^n can be written as $\exp(-\Sigma^* 2\sqrt{R_1^2 - y^2})$, where Σ^* is again given by Eq. (22). Integration of this probability over y , implicitly corresponding to a cosine current distribution at the interface I , gives, according to Eq. (4), the following:

$$T_{II} = \tau_{0,R_1}^{0,R_1} \circ \exp(-\Sigma^* 2\sqrt{R_1^2 - y^2}) \\ = 1 - (\frac{4}{3}\Sigma^* R_1) P_F(\Sigma^* R_1) , \quad (26)$$

which is analogous to Eq. (11).

The term that remains to be calculated for the interpebble Dancoff factor is the product $T_{iI}T_{Ii}$. This is the probability that a neutron leaving a fuel kernel isotropically reaches surface I of the pebble fuel zone, times the probability that a neutron isotropically leaving surface I (of another pebble) enters a fuel kernel somewhere in the fuel zone—both probabilities of course without moderator collisions and without passing through intermediate

kernels. The product $T_{ii}T_{ii}$ can now, analogously to the expression of the intrapebble Dancoff factor of Eq. (24), be determined as the infinite-medium Dancoff factor for the fuel kernel multiplied by the probability to escape from the fuel zone P_F times the nontransmission probability of the fuel zone $(1 - T_{ii})$ of the next pebble. This means that we have

$$T_{ii}T_{ii} = C_{\infty}^{fk} P_F(\Sigma^* R_1) [1 - T_{ii}] . \quad (27)$$

If this term is inserted into the expression for the interpebble Dancoff factor, given by Eq. (19), one obtains

$$C_{inter} = C_{\infty}^{fk} C_{\infty}^{FZ} \frac{P_F(\Sigma^* R_1) [1 - T_{ii}]}{1 - T_{ii} T_{io} T_{oi}} . \quad (28)$$

VII.C. Final Expression for the Dancoff Factor

The sum of the intrapebble [Eq. (24)] and the interpebble [Eq. (28)] Dancoff factor yields the total Dancoff factor, which becomes

$$C^{fk} = C_{\infty}^{fk} \left[1 - P_F(\Sigma^* R_1) + C_{\infty}^{FZ} \frac{P_F(\Sigma^* R_1) [1 - T_{ii}]}{1 - T_{ii} T_{io} T_{oi}} \right] , \quad (29)$$

where we recall [see Eq. (26)] that

$$T_{ii} = 1 - \left(\frac{4}{3}\Sigma^* R_1\right) P_F(\Sigma^* R_1) , \quad (30)$$

in which P_F is the first-flight escape probability from a sphere, given by Eq. (9), and its argument $\Sigma^* R_1$ is given by Eq. (25). Equation (29) shows that the Dancoff factor is equal to that of an infinite medium times the correction factor between the square brackets.

The infinite-medium Dancoff factor for the fuel kernel C_{∞}^{fk} is given by Eq. (12), where the transmission probabilities t_{io} , t_{oi} , and t_{oo} [Eqs. (5), (6), and (7)] are functions of (Σ_i^m, r_1, r_2) , which are the total macroscopic cross section of the spherical shell of the grain cell, and the inner and the outer radii of the grain cell. The infinite-medium Dancoff factor for the fuel zone is obtained in a similar way, but now the upper-case transmission probabilities T_{io} , T_{oi} , T_{oo} are functions of (Σ_i^M, R_1, R_2) , where Σ_i^M is the total macroscopic cross section of the spherical shell of the pebble cell, R_1 is the 2.5-cm radius of the fuel zone, and R_2 is the outer radius of the pebble cell. Equation (29) shows that if $T_{io} = T_{oi} = 1$, $T_{oo} = 0$, and hence $C_{\infty}^{FZ} = 1$, which implies that a neutron that leaves the fuel zone always reaches a neighboring fuel zone, the Dancoff factor is equal to that of the infinite medium, i.e., $C^{fk} = C_{\infty}^{fk}$. Furthermore, if the Dancoff factor for the fuel zone C_{∞}^{FZ} is zero, which means that a neutron cannot reach another fuel zone without collisions, the total Dancoff factor is equal to the intrapebble Dancoff factor [see Eq. (24)].

VIII. COMPARISON WITH MONTE CARLO RESULTS

The results obtained from the analytical formulas have been verified by Monte Carlo calculations performed with the MCNP-4A code.¹⁶ The Dancoff factor has been calculated as the number of neutrons entering a fuel kernel divided by the number of neutrons started from a fuel kernel boundary (uniformly and isotropically in the outward direction). The neutrons are followed until they enter a fuel kernel or they collide with a moderator nucleus.¹⁷ The Dancoff factor depends (besides on the geometry and the density of the moderator) on the total microscopic cross section of the moderator, which varies only with <1% from 0.2 eV to 10 keV. In the MCNP calculations the source neutrons have an energy of 100 eV, which corresponds to a total microscopic cross section of 4.7388 b. This yields for the graphite matrix material a macroscopic cross section of 0.4097 cm^{-1} , which implies that the radius of the pebble fuel zone is about equal to the mfp in the moderator.

In Secs. VIII.A through VIII.F the results of the analytical model are compared to those of the MCNP calculations, and the assumptions made in both methods are discussed. This is done for the infinite-medium Dancoff factor of the pebble fuel zone C_{∞}^{FZ} and that of the fuel kernel C_{∞}^{fk} . Thereafter, the intrapebble Dancoff factor C_{intra} as a function of the fuel zone radius is studied, and the Dancoff factor C^{fk} as a function of the outer radius of the pebble cell R_2 is investigated. Finally, the results of the total fuel kernel Dancoff factor C^{fk} as a function of the number of grains in the fuel zone are given for fuel kernels with radii of 100, 110, and 250 μm .

VIII.A. The Infinite-Medium Dancoff Factor for the Fuel Zone

In the analytical model the interpebble Dancoff factor is proportional to the infinite-medium Dancoff factor of the pebble fuel zone C_{∞}^{FZ} . The latter accounts for the probability that a neutron leaving the fuel zone surface isotropically in the outward direction reaches the fuel zone of another pebble without collisions.

Let a spherical *three*-region white-boundary pebble cell be the reference model for the stochastically stacked infinite pile of fuel pebbles. This pebble cell comprises the fuel zone ($R < 2.5 \text{ cm}$), the pebble shell ($2.5 < R < 3 \text{ cm}$), and the void belonging to the pebble ($3 < R < 3.52 \text{ cm}$) and gives after 16 million neutron histories a Dancoff factor of 0.4435 ± 0.0002 . A two-region cell, of which the spherical shell ($2.5 < R < 3.52 \text{ cm}$) contains a homogenized mixture of the void and the graphite of the pebble shell, yields (0.45337 analytically, 0.4532 ± 0.0002 MCNP), which is a deviation from the reference case of +2%. A two-region cell, of which the spherical shell is equal to the actual pebble shell ($2.5 < R < 3 \text{ cm}$) and where the void region is simply ignored, yields (0.44352 analytically, 0.4435 ± 0.0002 MCNP), which is within

the error margin (i.e., 0.05%) of the reference case. This means that in the case of the absence of moderator pebbles, the two-region Dancoff factor with neglect of the void region gives the best result compared to that of the reference case. This is of course only justified if the total macroscopic cross section of the void region is negligibly small, which is true if there is helium gas, even under high pressure, between the pebbles.

VIII.B. Homogenization of Coatings and Graphite Matrix

The number of coated particles per pebble N_{gr} has been varied from 5000 to 60 000 (step 5000) per pebble in the MCNP calculations. The outer radius of an equivalent spherical white-boundary grain cell r_2 is given by $r_2 = R_1/N_{gr}^{1/3}$, where we recall that R_1 is the 2.5-cm radius of the fuel zone. In the analytic model the coating layers surrounding each fuel kernel have been homogenized with the graphite matrix between the kernels. To estimate the error made by homogenizing the coating materials with the graphite, the Dancoff factor has been calculated for a two-region spherical grain cell and for a multiregion grain cell in which the coating layers are modeled explicitly. This has been done for grain cells (kernel radius of 250 μm) for which $N_{gr} = 5000$ and 60 000 and shows an underestimation for the two-region case of 0.3% and 0.01%, respectively.

VIII.C. The Infinite-Medium Dancoff Factor for a Fuel Kernel

The infinite-medium Dancoff factor for a fuel kernel has been calculated both analytically and with MCNP for grain densities corresponding to N_{gr} grains per fuel zone with the nominal volume of $\frac{4}{3}\pi(2.5)^3 \text{ cm}^3$. The analytical calculation embraces the evaluation of the expressions of Janssen and its rational approximation, as well as that of Lane. The MCNP calculations are performed for two geometries.

The first geometry is a cubic unit cell containing one fuel kernel only, with specular reflecting boundary conditions. This geometry is equivalent to an infinite rectangular lattice of cubic unit cells.

The second one is the infinite medium in which coated particles are randomly dispersed. The infinite medium was artificially created by a graphite sphere with isotropic reflecting boundary conditions in which 980 coated particles were randomly positioned. (This was due to limitations, namely, no more than 1000 cells, of the algorithm used in MCNP.) The radius of the sphere was chosen in such a way that the coated particle density was equal to the density of N_{gr} grains per fuel zone volume. To compare the MCNP results to those of the analytic models (no coating layers), we simply replaced the coating layers in the MCNP models by the graphite matrix. An MCNP calculation on a spherical two-region unit cell with

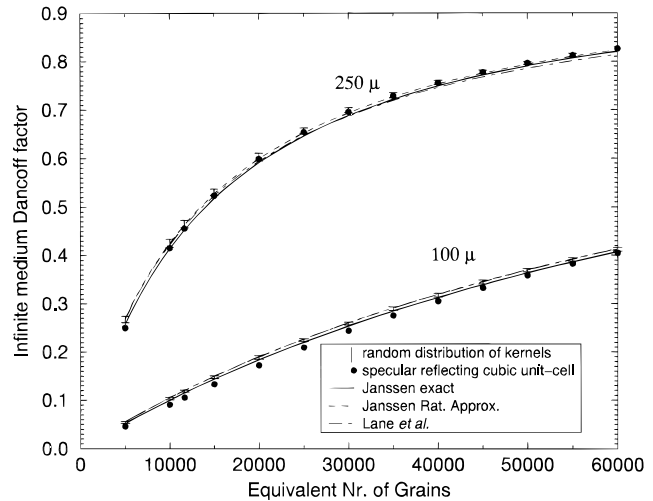


Fig. 5. The infinite-medium Dancoff factor C_{∞}^{jk} for the fuel kernel as a function of the equivalent number of grains, based on five methods. The equivalent number of grains (i.e., N_{gr}) on the horizontal axis corresponds to a grain density in the infinite medium that is equivalent to a density of $N_{gr}/[\frac{4}{3}\pi(2.5)^3] \text{ cm}^{-3}$, i.e., N_{gr} grains per nominal fuel zone of a pebble. The symbols (black circles and vertical lines) correspond to MCNP calculations, whereas the curves (solid, short-dashed, and long-dashed lines) correspond to analytical calculations. The solid, short-dashed, and long-dashed lines are calculated with Eq. (12), Eqs. (13) and (14), and Eqs. (13), (14), and (15), respectively.

isotropic reflecting boundary conditions has been discarded because this yields exactly the same results as the analytical expression of Janssen [Eq. (12)]. This has been verified for a number of N_{gr} values.

The results of the foregoing calculations are presented in Fig. 5. One can see that the Dancoff factors of the specular reflecting unit cell are in all cases lower than those of the random distribution of the coated particles. The relative difference is the largest for a small equivalent number of grains N_{gr} , i.e., low grain density, and for a small fuel kernel. The cubic unit cell with specular reflecting boundaries is equivalent to an infinite rectangular lattice of cubic unit cells, which means that channel effects will occur. In such a system the neutrons can stream in coated particle-free volumes, which results in an underestimation of the Dancoff factor. In the case of $N_{gr} = 5000$, the maximal relative differences of 7 and 18% for the 250- and 100- μm kernels, respectively, were found. Note, however, that in these cases the Dancoff factor itself is relatively low, which means that the error in the effective first-flight escape probability P_F^* due to the error in the Dancoff factor is relatively low.

The relative differences between the results of the random-distribution MCNP calculations and Janssen's exact expression of the Dancoff factor are maximal for $N_{gr} = 5000$ and amounts of 4 and 5% for the 250- and 100- μm kernels, respectively. The Dancoff factor values

of Lane et al. lie within the error margins of the random-distribution MCNP values, except for $N_{gr} > 20000$ in the case of the 250- μm kernel. This can be understood because the theory on which Lane's formula is based assumes a high dilution of the fuel kernels; i.e., the kernels occupy only a small part of the volume. Surprisingly, the rational approximation of Janssen's Dancoff factor fits better than Janssen's analytical expression and lies always within the error margins of the random-distribution MCNP results. This cannot be explained by physics considerations but rests mainly on lucky coincidence.

VIII.D. The Intrapebble Dancoff Factor as a Function of the Fuel Zone Radius

To verify the analytic expression of the intrapebble Dancoff factor [Eq. (24)], we have performed MCNP calculations on a single pebble with a varying fuel zone radius R_1 . The single pebble was modeled by placing an infinite rectangular lattice of cubic unit cells in a sphere with radius R_1 , as is shown in Fig. 6. A random distribution of coated particles was unfortunately not possible for this geometry because of limitations of the MCNP code. For the calculation of the intrapebble Dancoff factor, the spherical boundaries of the pebble-cell in Fig. 6 were transparent instead of reflecting. The Dancoff factor has been calculated through volume-averaging the

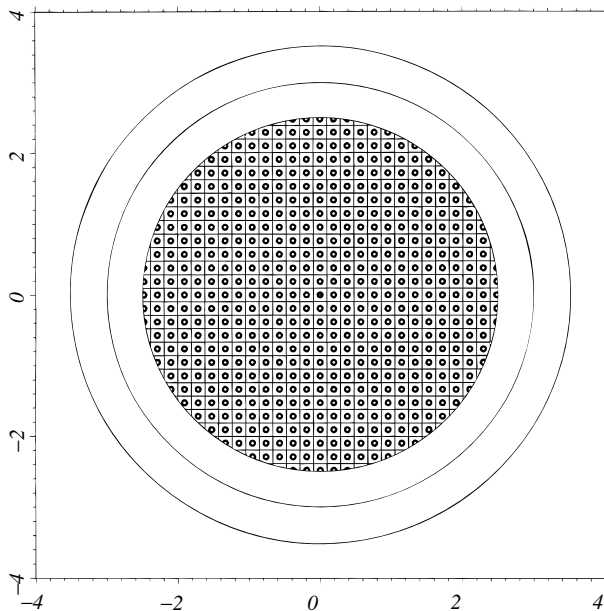


Fig. 6. Cross section through the midplane of the double-heterogeneous MCNP model of the pebble. It is composed of the fuel zone, containing a rectangular lattice of cubic unit cells, the 0.5-cm graphite shell, and the outer void shell. The outer spherical boundary is isotropically reflecting. The units on the axes are centimetres.

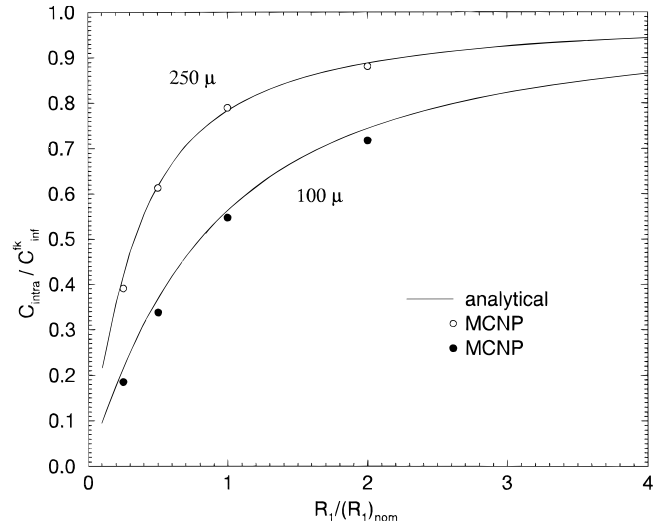


Fig. 7. The intrapebble Dancoff factor normalized to the infinite-medium Dancoff factor, $C_{intra}/C_{\infty}^{fk}$, as a function of the fuel zone radius, normalized to the nominal one of 2.5 cm, for two fuel kernel radii. The coated particle density is kept constant (namely, 30 000 coated particles per nominal fuel zone volume). For large fuel zone radii, the intrapebble Dancoff factor tends to the infinite-medium Dancoff factor.

Dancoff factors of individual coated particles at different radial positions, which is described in Sec. VIII.F.

Figure 7 shows the averaged intrapebble Dancoff factors, normalized to the infinite-medium fuel kernel Dancoff factor, $(C_{intra}/C_{\infty}^{fk})$, as a function of the fuel zone radius, normalized to the nominal 2.5-cm radius $[R_1/(R_1)_{nom}]$. This has been done for kernels with radii of 100 and 250 μm , at a constant coated particle density. This coated particle density corresponds to a loading of 30 000 coated particles in the standard ($R_1 = 2.5$ cm) fuel zone volume. The dots are the volume-averaged intrapebble Dancoff factors calculated by MCNP. The curves represent the analytical expression of the intrapebble Dancoff factor given by Eq. (24), which can be rewritten as $C_{intra}/C_{\infty}^{fk} = 1 - P_F(\Sigma^*R_1)$. This shows that for large R_1 values, the curves tend to unity, which implies that the intrapebble Dancoff factor becomes equal to the infinite-medium Dancoff factor. For the 100- μm kernel, the MCNP dots are lower than the analytical curve because of the previously mentioned channel effects in the rectangular lattice.

VIII.E. The Dancoff Factor as a Function of the Pebble Shell Thickness

To study the interaction between the fuel zones of different pebbles, we varied the outer radius of the pebble shell R_2 , while keeping the fuel zone radius constant, $R_1 = 2.5$ cm. The fuel zone of a pebble contains 30 000 coated

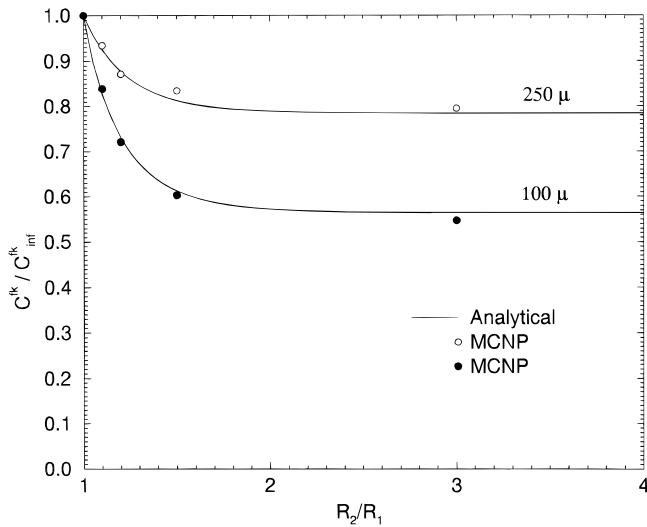


Fig. 8. The Dancoff factor, normalized to the infinite-medium Dancoff factor, C^{fk}/C_{∞}^{fk} , as a function of R_2/R_1 , for two fuel kernel radii. Here, R_2/R_1 is the outer radius of the pebble shell, normalized to the nominal 2.5-cm fuel zone radius R_1 . The fuel zone radius R_1 has been kept constant. The $R_2/R_1 = 1.2$ case corresponds to a standard pebble, without moderator pebbles. If $R_2/R_1 = 1$, i.e., zero pebble shell thickness, the Dancoff factor becomes equal to the infinite-medium Dancoff factor. In this case, the fuel zones of the pebbles are not separated by graphite from each other and notionally form an infinite medium. For very thick pebble shells ($R_2/R_1 \rightarrow \infty$), the Dancoff factor tends to the intrapebble Dancoff factor. In this case, a fuel zone is isolated from the other ones, and the interpebble Dancoff factor is therefore zero.

particles. Figure 8 shows the volume-averaged Dancoff factor, normalized to the infinite-medium Dancoff factor C^{fk}/C_{∞}^{fk} as a function of R_2/R_1 . The latter is the outer radius of the pebble shell R_2 divided by the fuel zone radius R_1 . For the standard pebble, $R_2 = 3$ cm, and hence, $R_2/R_1 = 1.2$. At this value the C^{fk}/C_{∞}^{fk} reads ~ 0.87 and 0.77 for the 250- and 100- μm kernels, respectively. For high R_2/R_1 values, the probability that a neutron that leaves the fuel zone of a pebble reaches the fuel zone of another pebble without collisions becomes negligible. This implies that the fuel zone Dancoff factor [C_{∞}^{FZ} in Eq. (29)] becomes zero. In that case, the interpebble Dancoff factor becomes zero, and hence, the total Dancoff factor becomes equal to the intrapebble Dancoff factor.

Note that the Dancoff factors for $R_2/R_1 \rightarrow \infty$ in Fig. 8 correspond to those at $R_1/(R_1)_{nom} = 1$ in Fig. 7. The $C_{intra}/C_{\infty}^{fk}$ values for the standard pebble read 0.78 and 0.56 for fuel kernels with radii of 250 and 100 μm , respectively. From this, one may infer that for the standard pebbles, the contributions of the intrapebble Dancoff factor to the total fuel kernel Dancoff factor read $\frac{0.78}{0.87} \cdot 100\% = 90\%$ and $\frac{0.56}{0.77} \cdot 100\% = 73\%$ for 250- and

100- μm kernels, respectively. Hence, the contributions of the interpebble Dancoff factor are 10 and 26%, respectively.

VIII.F. The Fuel Kernel Dancoff Factor for a Standard Pebble

Figures 9 and 10 show the total (intra- + interpebble) Dancoff factor of individual kernels as a function of their radial position. Each open symbol in Figs. 9 and 10 corresponds to the Dancoff factor of a single fuel kernel and is obtained after one million neutron histories in MCNP. The fuel zone is divided by the vertical dashed lines in ten regions with equal volumes. Note that about one-half of the number of coated particles is positioned in the outer spherical ($2 < R < 2.5$ cm) shell of the fuel zone.

Figure 6 shows that some of the fuel kernels are cut by the spherical ($R_1 = 2.5$ cm) surface. For these kernels no Dancoff factor could be calculated. Nevertheless, to obtain data in the vicinity of the boundary, for each set a point was added through extrapolation of the outer five MCNP points. The extrapolated data are represented by the filled symbols in Figs. 9 and 10. The Dancoff factor is calculated by volume-averaging the Dancoff factors of the individual kernels.

The volume-averaged Dancoff factor as a function of the number of grains in the fuel zone, with the kernel radius as a parameter, is shown in Fig. 11. The curves are obtained analytically through the evaluation of

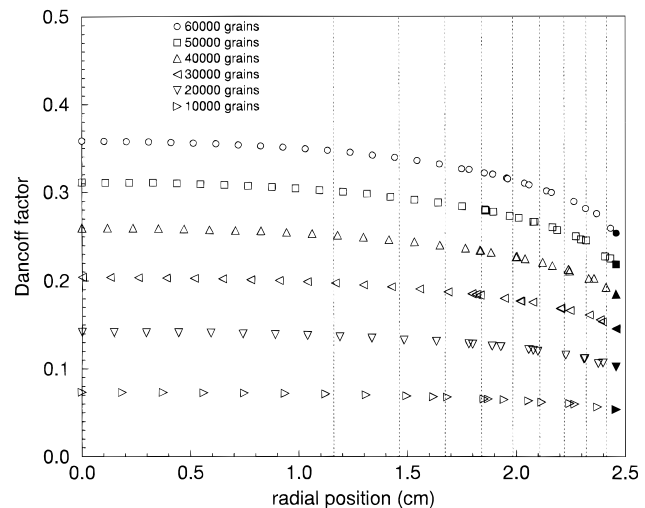


Fig. 9. Fuel kernel Dancoff factor as a function of the radial position in the pebble fuel zone for a fuel kernel with a 100- μm radius. Each point corresponds to one million MCNP neutron histories. The fuel zone is divided by the dashed vertical lines into 10 equivolumes. The filled symbols are extrapolated (second-order function) from the five outer MCNP points.

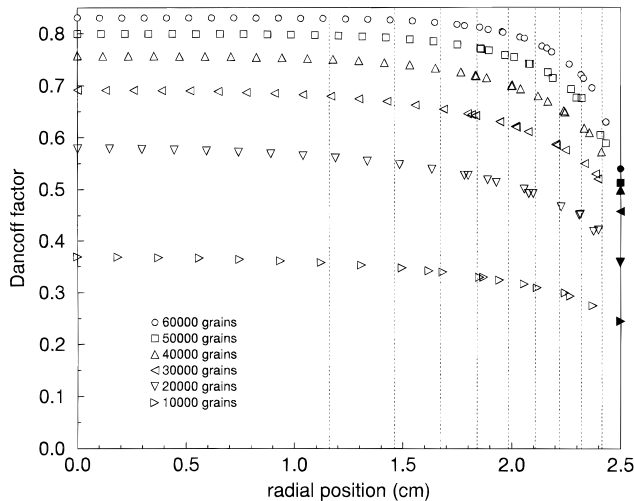


Fig. 10. Fuel kernel Dancoff factor as a function of the radial position in the pebble fuel zone for a fuel kernel with a 250- μm radius. Each point corresponds to one million MCNP neutron histories. The fuel zone is divided by the dashed vertical lines into 10 equivolumes. The filled symbols are extrapolated (second-order function) from the five outer MCNP points.

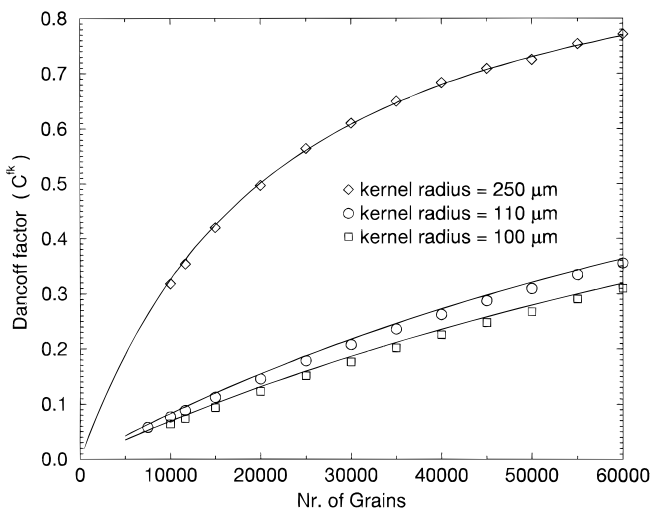


Fig. 11. The average fuel kernel Dancoff factor as a function of the number of coated particles (grains) in the fuel zone, with the fuel kernel radius as a parameter. Analytical (solid lines); MCNP (symbols).

Eq. (29), while the symbols correspond to the volume-averaged Dancoff factors calculated with MCNP. Each symbol in Fig. 11 is obtained through volume-averaging 20 to 35 Dancoff factors of individual kernels with different radial positions. The Dancoff factor of an individual kernel has been determined after one million neutron histories, which results, without variance reduction techniques in MCNP, in a statistical uncertainty of

$\sim 0.5\%$. One Dancoff factor calculation involves a CPU time of ~ 15 min on a 300-MHz Dec Alpha-2100. For example, if 28 individual kernel Dancoff factors are included for a particular volume-averaged Dancoff factor calculation, the total CPU time equals 7 h. This means that every symbol in Fig. 11 needed a CPU time of this order of magnitude. On the other hand, the evaluation of the analytical formula [Eq. (29)] by a FORTRAN code requires < 1 s.

The MCNP results are in good agreement with the analytical results for the 250- μm kernel. However, for the 100- and 110- μm kernels, the MCNP results are everywhere lower than the analytical results. The maximal differences amount to 0.01 in the absolute sense and 8% in a relative sense. The differences are probably caused by streaming of the neutrons in fuel kernel-free planes. These channel effects become relatively important if the spacing between kernels becomes larger, which is the case for small kernels and for low kernel densities.

IX. CONCLUSIONS

The Dancoff factor for fuel kernels embedded in a graphite matrix of infinite dimensions C_{∞}^{fk} has been calculated by three existing analytical methods and two MCNP calculations. The MCNP model, in which fuel kernels are randomly positioned in a graphite matrix, is the reference case. The C_{∞}^{fk} values obtained with the MCNP model, in which the fuel kernels are positioned in a rectangular cubic lattice, differ from those of the reference case by maximally 18%, which is caused by channel effects in the lattice. Janssen's analytical formula for C_{∞}^{fk} shows an underestimation of maximally 5% with the reference case. The maximal relative errors appear at low coated particle densities and for small kernel radii. In these cases the Dancoff factor is low, which implies that the effective escape probability is fortunately relatively insensitive to an error in the Dancoff factor. Janssen's rational expression, which is a simplification of the analytical one, gives results that are within the error margins of those of the reference case. The results of Lane's formula for low coated particle densities and low kernel diameters lie within the error margins of those of the reference case.

An analytical formula for the average Dancoff factor of fuel kernels embedded in the fuel zone of a pebble C^{fk} has been derived. It turns out that C^{fk} can be written as C_{∞}^{fk} times a correction factor, which accounts for the double heterogeneity of the system. This correction factor depends on the radius of the fuel zone of the pebble, the Dancoff factor of the pebble's fuel zone C_{∞}^{FZ} , the coated particle density in the fuel zone, and so on. The dependence of the correction factor with respect to the fuel zone radius and pebble shell thickness has been studied. The results of the analytical formula were in close agreement with the MCNP results.

The average Dancoff factor for the fuel kernel C^{fk} as a function of the number of grains in the fuel zone has been calculated analytically and with MCNP. This has been done for the standard pebble, with a 6-cm diameter and a 5-cm fuel zone diameter. In the case of a 250- μm fuel kernel radius, the methods are in good agreement. However, for the kernel radii of 100 and 110 μm , the MCNP calculation shows smaller C^{fk} values than those of the analytical method because of channel effects in the rectangular lattice used in the MCNP model.

The calculation of an averaged fuel kernel Dancoff factor by MCNP requires typically a CPU time of 7 h. Since it is, so far, impossible to model ten thousands of randomly positioned coated particles in the pebble fuel zone, one has to rely on coated particles arranged on a rectangular lattice, which introduces for small kernels and low coated particle densities errors due to channel effects. We recommend calculation of Dancoff factors with the analytical formula presented in this paper since this method consumes practically no CPU time, does not require the building of MCNP models, and gives very good results.

APPENDIX

A.I. DANCOFF FACTOR SENSITIVITY OF RESONANCE INTEGRALS AND OTHER PARAMETERS

In this appendix, we investigate whether an accurate calculation of the Dancoff factor is important to obtain core performance parameters of an HTR. First, the sensitivity of resonance integrals to the Dancoff factor is studied in a theoretical way. This is done for unbroadened ($T = 0$ K) resonances because this allows a rather simple analytical approach. It will turn out that the resonance parameters of each resonance determine a certain lump size for which the corresponding resonance integral is most sensitive to the Dancoff factor. As an example, we determine the radius of a spherical lump for which the Dancoff factor sensitivity of the important 6.7-eV resonance integral of ^{238}U is maximal. If the Dancoff factor equals 0.667, this radius appears to be identical to that of a UO_2 fuel kernel. The combination of the aforementioned radius and Dancoff factor corresponds to an HTR pebble that contains $\sim 38\,000$ coated particles. For this pebble, a double-heterogeneous unit-cell calculation was carried out, for which the Dancoff factor sensitivity of several reactor physics parameters was examined.

A.I.A. Analytical Approach

The narrow resonance infinite mass theory, in conjunction with Wigner's rational approximation for the

first-flight escape probability, yields for the resonance integral of an unbroadened ($T = 0$ K) resonance²

$$I = I_\infty \sqrt{\frac{\beta}{1 + \beta}}, \quad (\text{A.1})$$

where I_∞ is the infinite dilution resonance integral and

$$\beta = \frac{\sigma_p + (N_a \bar{l}_F)^{-1}}{\sigma_0} \frac{\Gamma}{\Gamma_\gamma}, \quad (\text{A.2})$$

where

σ_p = potential scattering cross section of the resonance absorber

σ_0 = total microscopic cross section at the resonance energy

Γ_γ = natural line width for capture

Γ = total natural line width.

The term $(N_a \bar{l}_F)^{-1}$ is commonly known as the microscopic escape cross section, in which N_a is the nuclide density of the resonance absorber and \bar{l}_F is the Dancoff-corrected (or effective) mean chord length of the fuel lump, which reads

$$\bar{l}'_F = \frac{\bar{l}_F}{1 - C}, \quad (\text{A.3})$$

where \bar{l}_F is the mean chord length of the fuel lump [$4 \times$ volume/surface (Ref. 5)] and C is the Dancoff factor. The Dancoff factor sensitivity coefficient of the resonance integral reads as follows:

$$\frac{C}{I} \frac{\partial I}{\partial C} = \frac{C}{2(1 - C)} \frac{\frac{\sigma_p}{\sigma_0} - \beta}{\beta(1 + \beta)}. \quad (\text{A.4})$$

A maximum of the sensitivity coefficient occurs if

$$\beta = \frac{\sigma_p}{\sigma_0} + \sqrt{\frac{\sigma_p}{\sigma_0} \left(1 + \frac{\sigma_p}{\sigma_0}\right)} \approx \sqrt{\frac{\sigma_p}{\sigma_0}}, \quad (\text{A.5})$$

where the approximation is valid for dominating resonances with $\sigma_p \ll \sigma_0$. Figure A.1 shows the Dancoff factor sensitivity coefficient $(C/I)(\partial I/\partial C)$, multiplied by $2(1 - C)/C$, as a function of $\beta(\sigma_p/\sigma_0)^{-1/2}$, with σ_p/σ_0 as parameter. Equations (A.2) and (A.3) show that $\beta = \sqrt{\sigma_p/\sigma_0}$ corresponds to

$$\bar{l}'_F = \frac{\bar{l}_F}{1 - C} \approx \frac{1}{N_A \sqrt{\sigma_p \sigma_0}} \frac{\Gamma}{\Gamma_\gamma}. \quad (\text{A.6})$$

This expression gives the effective mean chord length of a fuel lump for which the resonance integral of a particular resonance is most sensitive to the Dancoff factor.

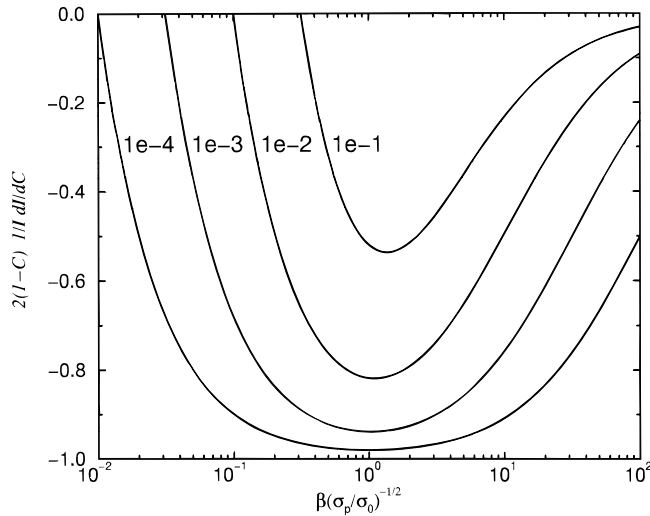


Fig. A.1. The Dancoff factor sensitivity coefficient of the resonance integral, $(C/I)(\partial I/\partial C)$, multiplied by $2(1 - C)/C$, as a function of $\beta(\sigma_p/\sigma_0)^{-1/2}$ with σ_p/σ_0 as parameter.

For $\beta = \sqrt{\sigma_p/\sigma_0}$, the Dancoff factor sensitivity coefficient for the resonance integral is maximal (in the absolute sense) and becomes

$$\left(\frac{C}{I} \frac{\partial I}{\partial C}\right)_{max} \approx -\frac{C}{2(1 - C)}. \quad (A.7)$$

This reveals that if the Dancoff factor is tending to unity, the resonance integral becomes more sensitive to the Dancoff factor. When $C = 0.667$ the Dancoff factor sensitivity coefficient of the resonance integral reads $(C/I)(\partial I/\partial C) = -1$. This means that if the Dancoff factor is overestimated by 1%, the resonance integral (and thus the group cross section that embraces the resonance) is underestimated by 1%. The 6.7-eV resonance of ^{238}U is characterized by $\Gamma_\gamma = 23.0 \times 10^{-3}$ eV, $\Gamma = 24.5 \times 10^{-3}$ eV, $\sigma_0 = 2.4 \times 10^4$ eV, and $\sigma_p = 11$ b. For a nuclide density of $0.021 \text{ b}^{-1} \cdot \text{cm}^{-1}$, Eq. (A.6) shows that the resonance integral of the mentioned resonance is most sensitive to the Dancoff factor if $\bar{l}_F/(1 - C) = 0.099$ cm. The radius of a spherical lump that corresponds to this chord length is equal to $r_F = \frac{3}{4}\bar{l}_F = 0.074 \times (1 - C)$. For $C = 0.667$, $r_F = 0.025$, which is identical to that of a UO_2 fuel kernel in an HTR. The aforementioned Dancoff factor refers to a pebble that contains ~ 38000 coated particles (with UO_2 kernels), which corresponds to 22.8 g HM per pebble.

A.I.B. Dancoff Factor Sensitivity of Several Parameters Obtained from Calculations

For the aforementioned HTR pebble (38000 UO_2 coated particles, 22.8 g HM per pebble, and 5.8 wt% enrichment), a double-heterogeneous cell calculation with

the SCALE code package has been performed. This involves, subsequently, a grain-cell calculation, in which the resonance shielding is carried out, and a pebble-cell calculation. The weighted fine-group cross sections of the grain cell are passed on to the eigenvalue calculation of the pebble cell. The validity of this two-step approach has been demonstrated in Ref. 17 by comparing several reactor physics parameters to those obtained by MCNP calculations. Moreover, the same document shows that single-heterogeneous calculations yield unsatisfying results. As the preceding theoretical analysis was based on unbroadened resonances, the calculation has been done at a temperature that was as low as possible, namely, 10 K. However, to obtain results for a realistic pebble as well, the same calculation was repeated with $T = 1200$ K.

Table A.I shows the change of some reactor physics parameters due to a reduction of the Dancoff factor by 10%. The Dancoff factor is denoted by C , σ_g^γ (in barns) is the shielded group cross section between 5.04 and 9.2 eV (containing the 6.7-eV resonance of ^{238}U), I_{res} (in barns) is the effective resonance integral (Nordheim method) of all resolved resonances lying between 1 and 677 eV, k_∞ is the infinite multiplication factor, p is the resonance escape probability, and C^* is defined as the ^{238}U capture rate divided by the ^{235}U fission rate. Table A.I shows that a reduction of the Dancoff factor by 10% causes an increase of σ_g^γ , also by almost 10%. This is in agreement with the Dancoff factor sensitivity coefficient of $(C/I)(\partial I/\partial C) = -1$ mentioned previously. For $T = 1200$ K, the changes of the parameters due to a reduction of C are slightly larger than those of $T = 10$ K. The changes in k_∞ and C^* amount to -3.7 and $+9\%$, respectively.

In conclusion, the Dancoff factor sensitivity coefficient of the resonance integral of a single resonance is determined by the size of the lump, the absorber density, the Dancoff factor, and the resonance parameters. The

TABLE A.I

Changes of Several Reactor Physics Parameters Due to a 10% Reduction of the Dancoff Factor

C	σ_g^γ	I_{res}	k_∞	p	C^*
Uniform $T = 10$ K					
0.6667	33.48	281.0	1.339	0.569	0.585
0.6	35.87	282.6	1.299	0.556	0.625
-10%	+7%	+0.6%	-3%	-2.4%	+7%
Uniform $T = 1200$ K					
0.6667	52.34	290.1	1.085	0.457	0.988
0.6	56.73	290.9	1.044	0.438	1.074
-10%	+8%	+0.3%	-3.7%	-4.2%	+9%

closer the Dancoff factor is to unity, the larger is this coefficient. The degree to which the resonance integral of a single resonance contributes to the total resonance integral determines the Dancoff factor sensitivity of the latter. Because both the moderator-to-fuel ratio and the total resonance integral determine the resonance absorption rate and thus p and k_{∞} , each system requires its own Dancoff factor sensitivity study.

ACKNOWLEDGMENTS

The authors wish to thank R. C. L. van der Stad for his help with the building of the MCNP input files.

REFERENCES

1. J. CHERNICK, "The Theory of Uranium Water Lattices," *Proc. Conf. Peaceful Uses of Atomic Energy*, Geneva, Switzerland, p. 603 (1955).
2. J. J. DUDERSTADT and L. J. HAMILTON, *Nuclear Reactor Analysis*, John Wiley & Sons, New York (1986).
3. L. W. NORDHEIM, "The Theory of Resonance Absorption," *Symp. Appl. Math.*, **11**, 58 (1961).
4. N. M. GREENE et al., "NITAWL-II, SCALE Module for Performing Resonance Shielding and Working Library Production," Oak Ridge National Laboratory (June 1989).
5. K. M. CASE, F. DE HOFFMANN, and G. PLACZEK, *Introduction to the Theory of Neutron Diffusion*, Los Alamos Scientific Laboratory (1953).
6. E. TEUCHERT, "Resonanzabsorption in einer zweifach heterogenen Anordnung kugelförmiger Brennelemente," *Nukleonik*, **11**, 68 (1968).
7. E. TEUCHERT and R. BREITBARTH, "Resonanzintegralberechnung für mehrfach heterogene Anordnungen," Juel-551-RG, Forschungszentrum Juelich (Sep. 1968).
8. G. F. KUNCIR, "A Program for the Calculations of Resonance Absorption," GA-2525, General Atomics (Sep. 1961).
9. L. W. NORDHEIM and G. F. KUNCIR, "A Program of Research and Calculations of Resonance Absorption," GA-2527, TID-4500, General Atomics (Aug. 1961).
10. R. K. LANE, L. W. NORDHEIM, and J. B. SAMPSON, "Resonance Absorption in Materials with Grain Structure," *Nucl. Sci. Eng.*, **14**, 390 (1962).
11. E. P. WIGNER et al., "Review of the Measurements of the Resonance Absorption of Neutrons by Uranium in Bulk," *J. Appl. Phys.*, **2**, 257, 260, 271 (1955).
12. S. M. DANCOFF and M. GINSBURG, "Surface Resonance Absorption in a Close-Packed Lattice," CP-2157 (Oct. 1944).
13. S. FEHÉR, J. E. HOOGENBOOM, P. F. A. DE LEEGE, and J. VALKÓ, "Monte Carlo Calculation of Dancoff Factors in Irregular Geometries," *Nucl. Sci. Eng.*, **117**, 227 (1994).
14. S. FEHÉR and P. F. A. DE LEEGE, "DANCOFF-MC, A Computer Program for Monte Carlo Calculation of Dancoff Factors in Irregular Geometries," IRI-131-95-003, Interfaculty Reactor Institute, Delft University of Technology (June 1995).
15. J. VALKÓ, J. E. HOOGENBOOM, and H. VAN DAM, "IRI Results for the LEU-HTR Proteus Computational Benchmarks, Part 1, Lattice Calculations for LEUPRO-1 & LEUPRO-2," IRI-131-94-010, Interfaculty Reactor Institute, Delft University of Technology (Apr. 1994).
16. "MCNP-4A: A General Monte Carlo Code for Neutron and Photon Transport," LA-7396-M, Rev. 2, J. F. BRIESMEISTER, Ed., Los Alamos National Laboratory (1986).
17. A. HOGENBIRK et al., "HTR-Proteus Benchmark Calculations," ECN-C-95-087, Netherlands Energy Research Foundation (Sep. 1995).
18. D. MATHEWS and R. CHAWLA, "LEU-HTR PROTEUS Computational Benchmark Specifications," TM-41-90-32, Paul Scherrer Institut, Labor für Reaktorphysik and Systemtechnik (Oct. 1998).
19. E. TEUCHERT, H. J. RUETTEN, and K. A. DE HAAS, "Rechnerische Darstellung des HTR-Modul Reaktors," Juel-2618, Forschungszentrum Juelich (May 1992).
20. K. G. HACKSTEIN, W. HEIT, W. THEYMANN, and G. KAISER, "Stand der Brennelemententechnologie für Hochtemperatur-Kugelhaufenreaktoren," *Atomenergie-Kerntechnik*, **47/3** (1985).
21. T. D. GULDEN and H. NICKEL, "Coated Particle Fuels," *Nucl. Technol.*, **35**, 206 (1977).
22. E. E. BENDE, "Transmutation of Plutonium in Pebble Bed Type High Temperature Reactors," *Proc. GLOBAL'97*, Yokohama, Japan, October 1997, p. 378 (1997).
23. H. BAIRIOT, L. AERTS, E. TRAUWAERT, and J. VAN GEEL, "Plutonium Coated Particles Development," *Nucl. Technol.*, **23**, 240 (1974).
24. R. M. WESTFALL, "Cosine Current Transmission Probabilities for Spherical Shells," *Trans. Am. Nucl. Soc.*, **18**, 147 (1974).
25. A. J. JANSSEN, "Enkele Opmerkingen over de Dancoff-factor," FYS-LWR-89-11, Netherlands Energy Research Foundation (Jan. 1990).
26. I. S. GRADSHTEYN and I. M. RYZHIK, *Table of Integrals, Series, and Products*, Academic Press, New York (1980).
27. "SCALE—Material Information Processor," NUREG/CR-0200, ORNL/NUREG/CSD-2/R4, RSIC/CCC-545, Oak Ridge National Laboratory.
28. J. R. KNIGHT, "SUPERDAN Computer Programs for Calculating the Dancoff Factor of Spheres, Cylinders and Slabs," ORNL/NUREG/CSD-TM-2, Oak Ridge National Laboratory (Mar. 1978).